Journal of Statistical Physics, Vol. 128, Nos. 1/2, July 2007 (© 2007)
DOI: 10.1007/s10955-006-9238-0

Loss- and Gain-of-Function Mutations in Cancer: Mass-action, Spatial and Hierarchical Models

Natalia L. Komarova[1]

Received March 24, 2006; accepted October 9, 2006
Published Online December 2, 2006

We study the stochastic dynamics of the two most common patterns in cancer initiation and progression: loss-of-function and gain-of-function mutations. We consider three stochastic models of cell populations with a constant size: a mass-action model, a spatial model and a hierarchical model. For gain-of-function mutations, we calculate the probability of mutant fixation starting from one mutant cell. For loss-of-function mutations, we calculate the rate of production of double-hit mutants. It turns out that the results are different in all models. This suggests that simple mass-action models are often misleading when studying cancer dynamics. Moreover, our results also allow us to think about various types of tissue architecture and its protective role against cancer. In particular, we show that hierarchical tissue organization lowers the risk of cancerous transformations. Also, cellular motility and long-range signaling can decrease the risk of cancer in solid tissues.

KEY WORDS: Tumor suppressor genes, oncogenes, homeostatic control, stem cells, Moran process, stochastic tunneling, nearest neighbor interactions, finite branching process

1. INTRODUCTION

Cancer is a very complex process which can be studied on several spatial scales. Subcellular, molecular processes such as mutations, chromosomal changes, as well as intracellular signaling, happen on the *subcellular* scale. They are responsible for malignant transformations that turn a healthy cell into a malignant one. Cells in an organ are not independent of each other. They interact by means of direct cell-to-cell signaling as well as through the process of selection; they compete for space and nutrients. The resulting dynamics happen on the *cellular* level. The

[1] Departments of Mathematics, University of California, Irvine, CA 92697, USA; e-mail komarova@math.uci.edu.

macroscopic description, or the *organismal* scale, is appropriate when studying a larger population of cancerous cells, which can be viewed as a continuum. The largest scale is the *inter-organismal*, or population scale. There, people study the epidemiology and statistics of cancer.

In this paper we will focus on the impact of intracellular processes on the next level of dynamics, the cellular level. We will examine the result of mutations and other molecular changes inside cells on the cellular dynamics of cancer initiation and progression. We will study the spread of mutated cells through a population of wild-type cells and investigate how the fitness properties of the mutants affect the probability and timing of mutant takeover.

1.1. Loss- and Gain-of-Function Mutations

By means of statistical analysis of the cancer retinoblastoma, Alfred Knudson came up with the "two-hit" hypothesis as a genetic mechanism of carcinogenesis.[16] Since then a two-hit mechanism has been found responsible for many cancers. The genes involved are termed *tumor suppressor genes* (TSG).[36,37] They are defined as genes whose protein product limits tumor growth (by inhibiting cellular growth or inducing cell death). When a TSG is mutated, the mutant allele acts as a recessive: as long as the cell contains a normal allele, tumor suppression continues. More than a hundred TSGs have been discovered. For example, inactivation of the Rb gene leads to retinoblastoma, and inactivation of the APC gene is one of the earliest events in colorectal cancers. Other tumor suppressor genes are p53 (it is inactivated in many cancers), and BRC1 and BRC2 (breast cancer).[36]

The inactivation of a TSG is an example of a "loss-of-function" mutation.[33] Upon the first hit, when one of the copies of the TSG is inactivated, the fitness of the cell is similar to that of wild-type cells, because there is still one functional copy of the TSG remaining. However, a second inactivating hit in such a cell will lead to a drastic increase in the fitness as the TSG is now completely turned off.

Another common event is a "gain-of-function" mutation (see e.g. Ref. 33) which activates an *oncogene.* An oncogene is a modified gene that increases the malignancy of a tumor cell, e.g. the RAS oncogene found in colon cancer,[36] and the Brc-Abl fusion gene found in chronic myeloid leukemia.[13] The corresponding cells have an advantageous phenotype and have a tendency to expand.

1.2. Mutation-Selection Diagrams

We can represent the process of a loss-of-function mutation by means of a mutation-selection diagram:

$$A_{(1)} \to^{u} B_{(r)} \to^{u_1} C_{(R)}. \tag{1}$$

Here, type "A" is the wild type, type "B" represents the phenotype with one copy of the TSG inactivated (and the fitness r is similar or equal to that of type "A"), and type "C" has no functioning copies of the TSG, and an increased fitness, $R > 1$. We will refer to diagram (1) as the two-species model.

Processes described by diagram (1) can also be discussed in the context of the phenomenon of genetic instability.[22] If the first mutation, "A" $\rightarrow$ "B," is an event by which a cell acquires an unstable, *mutator* phenotype,[24,25] then the fitness of type "B" (the unstable cells) could be equal to that of the wild type. Alternatively, it could be lower,[19,21] because instability results in a higher chance to create non-viable offspring, and thus confers a disadvantage to the cell. However, the next event could happen at an accelerated rate, u_1, and leads to a fast generation of type "C" cells, which may have a selective advantage.

A gain-of-function mutation (e.g. the activation of an oncogene) can be described by the following simple diagram:

$$A_{(1)} \rightarrow^{u} B_{(r)}. \tag{2}$$

Here, type "A" is the "wild type," "B" is the type with a mutated oncogene, and u is the rate of mutation. The fitness of type "B" is denoted by r and it is larger than the fitness of type "A" (which is normalized to 1).

Diagrams (1) and (2) of course do not uniquely define the dynamics of the populations of cells. To make the description complete, we need to make assumptions on the underlying processes of cellular birth, death and mutations.

1.3. Three Stochastic Models

We assume that the size of the cell population remains constant, and consider three different models of homeostasis maintenance: (1) a mass-action model, (2) a spatial model and (3) a hierarchical model. The first model assumes a spatially homogeneous cellular population. The second model includes spatial locations of cells. Unlike the first two models, the third model distinguishes between stem and daughter cells (with spatial locations included implicitly, inasmuch as the cell's position in the cell hierarchy correlates with its spatial location).

We will ask two specific questions: (i) For gain-of-function mutations, what is the rate of fixation of mutants depending on their relative fitness and the total number of cells in the constant population? (By fixation we mean the absorbing state where all cells are mutant). (ii) For loss-of-function mutations, what is the rate of generation of double-hit mutants, depending on the fitness of single-hit mutants, mutation rates and the total number of cells?

We will show that cellular dynamics of loss-of-function and gain-of-function mutations is quite different in the three models, and suggest how this relates to the protective function of tissue architecture.

This paper is organized as follows. In Sec. 2 we describe the mass-action model, in Sec. 3 we introduce the spatial model, in Sec. 4 we study the hierarchical model, and in Sec. 5 we compare the dynamics corresponding to the different models. Section 6 contains discussion.

2. A MASS-ACTION MODEL

Inspired by Knudson's two-hit hypothesis,[16] Moolgavkar[29] has created a mathematical two-hit model which describes the probability of accumulation of two mutations in a population of cells. Initially the theory was limited to an exponentially growing (on average) population, and later it was modified to include other laws of overall population growth,[12] and extended to multi-hit scenarios.[27] For two hits (of which the second one is highly advantageous) some interesting analytical results on the hazard function have been obtained.[9] Many other stochastic models have been proposed, including Refs. 23, 30, 34, 35. A common feature of all these models is that cells are assumed to interact with one another regardless of their spatial location. We term such models "mass-action models." In this section, we will review the mass-action model of Ref. 19, which assumes a population with a constant number of cells.

2.1. Model Definition

Each of the N cells in a spatially homogeneous population belongs to one of the three types, "A," "B" or "C." The dynamics is governed by a stochastic process described below. The cells can divide (possibly with mutations) and die. The rate of cellular division is governed by their relative fitness. The fitness is the same for all cells of a given type; it is different for cells of different types. We take the fitness of type "A" to be 1 (this sets the time-scale of the process). Relative to this, the fitness of type "B" is r and the fitness of type "C" is R. We assume that $R \gg 1$, and r can be smaller or equal to 1. The mutation network is given by diagram (1). Note that we do not allow back mutations. Each time a cell dies, it is immediately replaced by means of a cell division, so that the population size is kept constant. Cells are chosen for death at random. Reproduction happens proportional to the cells' fitness.

We say that the system is in the state j, $0 \leq j \leq N$ if (1) the number of cells of type "B" is equal to j and (2) there are no cells of type "C" present. In order to account for the production of double-mutants (cells of type "C"), we add state $j = E$ to the system. $j = E$ means that there is at least one cell of type "C" in the population. We assume that this state is absorbing, that is, once one mutant of type "C" is produced, it will take over the population (this is equivalent to the assumption $R \to \infty$).

The stochastic process which governs the cellular dynamics is a Markov, continuous-time, discrete state-space process. It is a linear birth-death process with mutations; formal analyses of aspects of linear processes and several examples can be found in e.g. Ref. 15. During an infinitesimally short time-interval, Δt, one of the following processes will happen:

- Transition $j \to j+1$ with probability $\Delta t\, P_{j\to j+1}$, where

$$P_{j\to j+1} = \frac{N-j}{N}\frac{rj(1-u_1)}{N-j+rj} + \frac{N-j}{N}\frac{(N-j)u}{N-j+rj}, \quad 0 \le j \le N-1. \tag{3}$$

  Here, the first term is the probability for a cell of type "A" to be chosen for death times the probability for a cell of type "B" to be chosen for reproduction and reproduce faithfully. The second term is the probability of death of a type "A" cell times the probability for a cell of type "A" to reproduce with a mutation.
- Transition $j \to j-1$ with probability $\Delta t\, P_{j\to j-1}$, where

$$P_{j\to j-1} = \frac{j}{N}\frac{(N-j)(1-u)}{N-j+rj}, \quad 1 \le j \le N. \tag{4}$$

  Here, we multiply the probability of a cell of type "B" to die by the probability of a cell of type "A" to reproduce without a mutation.
- Transition $j \to E$ with probability $\Delta t\, P_{j\to E}$, where

$$P_{j\to E} = \frac{rju_1}{N-j+rj}, \quad 0 \le j \le N, \tag{5}$$

  which is just the probability for a cell of type "B" to be chosen for reproduction and to reproduce with a mutation. It does not matter which cell type is chosen for death in this case. We also have
- $E \to E$ with probability 1 and $j \to j$ for $j \neq E$ with probability $1 - \Delta t(P_{j\to j+1} + P_{j\to j-1} + P_{j\to E})$.

All other transitions have zero probability. These transition rates completely define the Markov process.

2.2. Probability of Mutant Fixation in the Two-Species Model

We start our analysis with a review of simple but important results on the dynamics of gain-of-function mutations, see the two-species model of diagram (2).

Let us first consider a system where all mutations are suppressed ($u = 0$). We start from one cell of type "B" ($j = 1$). The states reachable from $j = 1$ are $j \in \{0, 1, \ldots, N\}$, and there are two absorbing states: $j = 0$ (extinction of type

"B") and $j = N$ (fixation of type "B"). The first question we would like to address is the following: what is the probability that starting from one mutant of type "B," the system will get absorbed in state $j = N$? It can be calculated by standard methods. Let us suppose that π_i is the probability to get absorbed in state N starting from state i. We have

$$\pi_i = \frac{1 - 1/r^i}{1 - 1/r^N}. \tag{6}$$

In the following analysis we will use the quantity

$$\pi_1 \equiv \rho(r) = \frac{1 - 1/r}{1 - 1/r^N}. \tag{7}$$

We have $\rho(r) = 1/N$ for $r = 1$, which can also be shown from simple symmetry considerations.

Next, let us include the possibility of mutations from "A" to "B," that is, $u > 0$. There is only one absorbing state in this system, $j = N$. The time of absorption can be approximated by

$$T_{abs} = (u\rho)^{-1}. \tag{8}$$

Indeed, the average number of new mutations arising in a unit time is given by u. Out of these, the fraction ρ, Eq. (7), will proceed to fixation. If mutations are rare, then the production of new mutants can be considered independent of the dynamics of the existing mutants. Therefore, the rate of fixation is a composite of the production of mutations, u, and the probability for each mutant to reach fixation, ρ. The typical time of absorption is the reciprocal of that.

Formula (8) holds if the mutation rate is sufficiently small (or, if the population size is not too large). The precise condition for this was derived in Ref. 19. This condition is equivalent to the statement that the characteristic time for a mutant to reach fixation is a lot smaller than a characteristic time of mutant production. For neutral mutants, such that $|1 - r| \ll 1/N$, this amounts to

$$N \ll N_{cg} = 1/u, \tag{9}$$

and for disadvantageous mutants, such that $r < 1$ and $|1 - r| \gg 1/N$, the condition is weaker,

$$N \ll N_{cg} = \frac{r^{-(N-1)}}{u}. \tag{10}$$

Here, the subscript "*cg*" stands for "coarse-grained"; this term will be explained below. Note that condition (9) is a sufficient condition for both cases; condition (9) follows from condition (10) for r close to one.

2.3. Three-Species Dynamics: A Coarse-Grained Description

Let us now consider the dynamics of loss-of-function mutations, the three-species model of diagram (1). We will investigate the process of fixation in the state E, which is the only absorbing state of system (1).

Note that the full stochastic system under consideration evolves in a large state space, $j \in \{E, 0, 1, \ldots, N\}$. The dynamics is governed by the $(N+2) \times (N+2)$ transition matrix defined in Eqs. (3–5). It is possible to show that under certain circumstances, the dynamics can be approximately described by means of a reduced system with only a small number of "long-lived," homogeneous states.

Let us denote the probability to find the system in state $j = 0$ by $x_0(t)$, the probability to find it in state $j = N$ by $x_1(t)$ and the probability to find it in state $j = E$ by $x_2(t)$. Here, x_0 and x_1 correspond to the *all* "A" and *all* "B" states, and x_2 corresponds to the *at least one cell of type* "C" state. The subscripts refer to the number of mutations (0, 1 or 2) that each type of cells has.

It is possible to show that if the mutation rate is sufficiently small, condition (10), we have

$$x_0 + x_1 + x_2 = 1 - O(1/N). \tag{11}$$

In other words, if mutations are rare, the system spends most of the time in one of the three long-lived states. This suggests the following way to simplify the analysis. We describe the dynamics as a sequence of Markovian hops between states x_0, x_1 and x_2, with some (time-constant) rates, $R_{0\to1}$, $R_{1\to2}$ and $R_{0\to2}$. We will refer to this simplified description as the *coarse-grained* dynamics. The Kolmogorov-forward equation for this reduced, coarse-grained system, reads:

$$\dot{x}_0 = -R_{0\to1}x_0 - R_{0\to2}x_0, \tag{12}$$

$$\dot{x}_1 = R_{0\to1}x_0 - R_{1\to2}x_1, \tag{13}$$

$$\dot{x}_2 = R_{1\to2}x_1 + R_{0\to2}x_0, \tag{14}$$

with the initial condition

$$x_0(0) = 1, \quad x_1(0) = x_2(0) = 0.$$

Note that since we only have unidirectional mutations, no positive rates other than $R_{0\to1}$, $R_{1\to2}$ and $R_{0\to2}$ can exist among these three states. System (12–14) is a simple linear system of ODEs, with constant coefficients. Note that here and in what follows we use the *generation* time-scale. That is, we scale time with N, the total number of cells, so that we have on average N cell-divisions per time-unit. This is equivalent to introducing a new time variable $\tilde{t} = Nt$; in what follows the tildes are omitted.

From an intuitive standpoint, the simplification procedure leading to system (12–14) is justified as long as the transitions among intermediate states (states

other than $x_{0,1,2}$) are much faster than the time scale of interest, that is, the time-scale of transition between states in the reduced state-space, x_0, x_1 and x_2. Let us give an intuitive derivation of condition (9) for the coarse-grained description to be valid in the case of neutral mutations (the argument can be easily extended to mutants with fitness $r < 1$, inequality (10)). Let us set $u_1 = 0$ for the moment. The rate of mutant production is Nu (again, the time has been scaled by N). The rate of production of successful mutants is $Nu\rho$, and thus the typical waiting time until fixation is $T_{\text{wait}} = (Nu\rho)^{-1}$. On the other hand, it takes about $T_{\text{fix}} = N$ time-steps for a mutant of type "B" to get fixated. Taking $\rho = 1/N$ in the neutral case, we can see that $T_{\text{wait}} \gg T_{\text{fix}}$ is equivalent to condition (9). Turning the second mutations rate back on, $u_1 > 0$, we can see that condition $u_1 \ll 1$ is enough to ensure that transition $x_0 \to x_2$ is slow. The formal analysis involves comparing eigenvalues of the corresponding transition matrices; for details we refer to Appendix C and D in Ref. 19.

Constants $R_{0\to1}$, $R_{1\to2}$ and $R_{0\to2}$ in system (12–14) characterize the transitions between the three long-lived states. The first two rates, $R_{0\to1}$, $R_{1\to2}$, are found easily. Indeed, the rate $R_{0\to1}$ is given by

$$R_{0\to1} = Nu\rho, \tag{15}$$

where the constant probability of mutant fixation, ρ , appears in formula (8). The rate $R_{0\to1}$ reflects the production of mutants followed by their successful fixation. The rate $R_{1\to2}$ is obtained similarly, except the probability of fixation of mutants of type "C" is considered to be equal to 1, yielding

$$R_{1\to2} = Nu_1. \tag{16}$$

The processes reflected in constants $R_{0\to1}$ and $R_{0\to2}$ are shown in Fig. 1(a). First the system gets into the all "B" state, after which another mutation brings it to the all "C" state. We will call this scenario a genuine *two-step process*.

The third constant appearing in system (12–14), $R_{0\to2}$, has the meaning of *tunneling*: the system reaches the all "C" state without first pausing at the all "B" state, see Fig. 1(b).

2.4. The Tunneling Rate in the Mass-Action Model

In order to calculate the rate at which tunneling occurs, we will use the approximation of a doubly-stochastic process. Starting with all cells in state "A," let us denote the probability to have a double mutant at time t as $P_2(t)$. We will view the stochastic process as a sequence of subprocesses, each of which is a mutation generating one cell of type "B," and its subsequent evolution. Each such subprocess describes the lineage starting with a single mutant of type "B." We will assume that these lineages are independent, that is, the total number of mutants of type "B" is small compared to N. This assumption holds most of the time unless

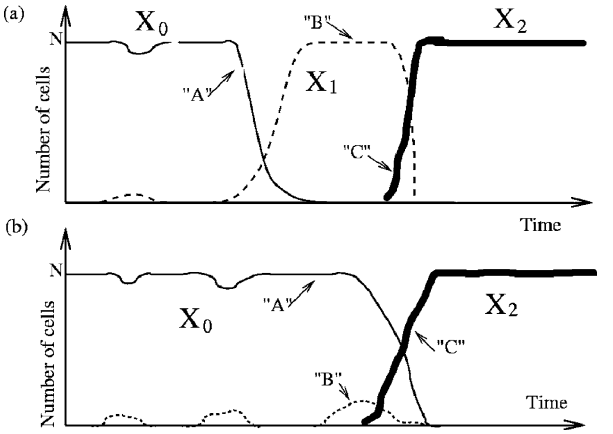

Fig. 1. Typical dynamics of cells. The thin solid line corresponds to the number of cells of type "A," the dashed line is type "B" and the thick solid line is type "C." (a) A two-step process, where fixation of type "B" is followed by fixation of type "C," (b) Tunneling, where fixation of type "B" does not occur.

a mutant of type "B" reaches fixation, in which case we have a two-step process with rates $R_{0\to 1}$ and $R_{1\to 2}$. The exact condition for tunneling to be important is given below. If $P_1(t)$ is the probability to obtain a double mutant by time t within a lineage starting from 1 cell of type "B," then we have, under the assumption of independence of different lineages,

$$P_2(t) = 1 - \exp\left[-u_N \int_0^t P_1(t')dt'\right] \tag{17}$$

(see e.g. Ref. 31 for a derivation). The probability $P_1(t)$ was calculated by Ref. 19 and then by Ref. 14. The function $P_1(t)$ is a monotonically increasing function of time, which starts off as a linear function and then reaches a saturation level, P_1^∞. It turns out that it is the saturation level that gives the main contribution to the integral in (17), see below. Here we develop a concise and instructive method for calculation of P_1^∞, which we will later use for the spatial model.

For the number of cells of type "B" we have a one-dimensional Markov process. The state $j = 0$ corresponds to extinction, which is an absorbing state. An additional absorbing state, $j = E$, is included to indicate that a cell of type "C" has been produced. The transition probabilities are given by formulas (3), (4) and (5). The main feature of tunneling is that fixation of the type "B" does not occur. In fact, for most realizations, the number of cells of type "B" is small compared to

N. Using this fact, the expressions for transition rates can be simplified to yield,

$$P_{j\to j+1} = \lambda j, \quad P_{j\to j-1} = \mu j, \quad P_{j\to E} = \beta j. \tag{18}$$

These transition coefficients are obtained by taking the highest order term in the expansion of coefficients (3), (4) and (5) in terms of the small parameter j/N:

$$\lambda = r(1-u_1), \quad \mu = 1, \quad \beta = u_1 r.$$

Note that an extra term N contained in the denominator in formulas (3), (4) and (5) is canceled by using the generation time-scale. For generality purposes we will carry out all the calculations for general constant values of λ, μ and β.

Let us denote by $\xi_i(t)\Delta t$ the probability to jump to state E during the time interval $(t, t+\Delta t)$, given that at time 0 we are in state i. This function satisfies the following equation:

$$\dot{\xi}_i = \lambda i \xi_{i+1} + \mu i \xi_{i-1} + \beta i \xi_E - i(\lambda+\mu+\beta)\xi_i, \quad 2 \le i.$$

The boundary condition is given by

$$\dot{\xi}_1 = \lambda \xi_2 + \mu \xi_0 + \beta \xi_E - (\lambda+\mu+\beta)\xi_1,$$

with $\xi_0(t) = \xi_E(t) = 0$. The initial condition is

$$\xi_i(0) = i\beta. \tag{19}$$

Let us take the Laplace transform of the ODE, where

$$\mathcal{L}\xi_i(t) = f_i(s).$$

Using $\mathcal{L}\dot{\xi}_i = s f_i - \xi_i(0)$, we obtain the following system of equations,

$$i[\lambda f_{i+1} + \mu f_{i-1} - (\lambda+\mu+\beta) f_i] - f_i s = -i\beta, \quad i > 1, \tag{20}$$

$$[\lambda f_2 - (\lambda+\mu+\beta) f_1] - f_1 s = -\beta. \tag{21}$$

In order to obtain $P_1(t)$, the mutation probability in each lineage, we would need to find $f_1(s)$ (we start from one cell of type "B"), and evaluate $\mathcal{L}^{-1}[f_1(s)/s]$. Indeed, the cumulative probability $P_1(t)$ is related to the function $\xi_1(t)$ as $\xi_1 = \frac{dP_1}{dt}$. Therefore their Laplace transforms differ by a factor s. However, it is the value $P_1^\infty = \lim_{t\to\infty} P_1(t)$ that gives the main contribution to probability (17)), see below. This value is given simply by $P_1^\infty = f_1(0)$. We can solve system (20–21) analytically in the special case where $s = 0$. We have,

$$\lambda f_{i+1} + \mu f_{i-1} - (\lambda+\mu+\beta) f_i = -\beta, \quad i > 1, \tag{22}$$

$$[\lambda f_1 - (\lambda+\mu+\beta) f_1] = -\beta. \tag{23}$$

The general solution is given by

$$f_i = 1 + A\alpha_-^i + B\alpha_+^i,$$

where the numbers $\alpha_\pm$ are the roots of the quadratic equation, $\lambda\alpha^2 - (\lambda + \mu + \beta)\alpha + \mu = 0$. We can see that $\alpha_+ > 1$ and $0 < \alpha_- < 1$. Using the boundary condition for f_1 and boundedness of f_i, we obtain $A = -1$ and $B = 0$, such that $f_i = 1 - \alpha_-^i$, and

$$f_1(0) = 1 - \frac{1}{2\lambda}(\lambda + \mu + \beta - \sqrt{(\lambda + \mu + \beta)^2 - 4\lambda\mu}).$$

We will consider the following two limiting cases:

- The mutant "B" is negatively selected, that is, $\mu > \lambda$ and $\beta(\lambda + \mu) \ll (\lambda - \mu)^2$. In this case, $\alpha_- = 1 - \frac{\beta}{\mu - \lambda}$ and $f_1(0) =$

$$P_1^\infty = \frac{\beta}{\mu - \lambda} = \frac{ru_1}{1 - r}. \tag{24}$$

- The mutant "B" is neutral, that is, $\beta(\lambda + \mu) \gg (\lambda - \mu)^2$. In this case we obtain $\alpha_- = \sqrt{\beta/\lambda}$ and the tunneling rate,

$$P_1^\infty = \sqrt{\beta/\lambda} = \sqrt{u_1}. \tag{25}$$

In order to estimate expression (17), we need to know the time-scale of change of the function $P_1(t)$. It approaches its saturation level around the time $t_c \sim \sqrt{\beta\lambda}$ in the case of neutral mutants and $t_c \sim \mu - \lambda$ in the case of disadvantageous mutants (see the derivation in Ref. 38 or in Ref. 17).

The time-scale of interest is when the expression in the exponent of (17) becomes of the order one,

$$u_N \int_0^t P_1(t')\, dt' \sim 1.$$

Since $P_1(t) \leq P_1^\infty$ for all values of t, we have

$$t P_1^\infty > \int_0^t P_1(t')\, dt' \sim \frac{1}{uN},$$

which gives us

$$t > \frac{1}{uN P_1^\infty}.$$

For neutral mutants this yields $t > \sqrt{\lambda/(uN\beta)}$, and for disadvantageous mutants we have $t > (\mu - \lambda)/(uN\beta)$. In both cases we can see that because of conditions (9) or (10), we have for the time-scale of interest,

$$t \gg t_c. \tag{26}$$

Therefore the function $P_1(t)$ under the integral in Eq. (17) can be replaced by its saturated value:

$$P_2(t) = 1 - e^{-uNP_1^{\infty}t}.$$

This means that the rate of tunneling, $R_{0\to 2} = NuP_1^{\infty}$ in Eqs. (12–14) is given by

$$R_{0\to 2} = Nu\left[1 - \frac{1}{2\lambda}(\lambda+\mu+\beta) - \sqrt{(\lambda+\mu+\beta)^2 - 4\lambda\mu}\right]. \tag{27}$$

We can simplify this expression in the following limiting cases:

- Disadvantageous mutants "B," that is, $\mu < \lambda$ and $\beta(\lambda+\mu) \ll (\lambda-\mu)^2$. In this case, we have

$$R_{0\to 2} = uN\frac{\beta}{\mu-\lambda} = \frac{uu_1rN}{1-r}. \tag{28}$$

- Neutral mutants "B," that is, $\beta(\lambda+\mu) \gg (\lambda-\mu)^2$. We have

$$R_{0\to 2} = uN\sqrt{\beta/\lambda} = u\sqrt{u_1}N. \tag{29}$$

Tunneling is the dominant process if the inequality $R_{0\to 1} \ll R_{0\to 2}$ holds,[38] which is equivalent to condition $\rho \ll P_1^{\infty}$. A simple calculation shows that this can be rewritten in the following way:

$$N \gg N_{\text{tun}}, \tag{30}$$

where in the case of disadvantageous mutants,

$$N_{\text{tun}} = \frac{\log u_1 + 2\log[r/(1-r)]}{\log r}, \tag{31}$$

and in the case of neutral mutants,

$$N_{\text{tun}} = \frac{1}{\sqrt{u_1}}. \tag{32}$$

2.5. Mass Action Model: Beyond Tunneling

Let us now investigate what happens when condition $N \gg N_{cg}$ breaks down. For these very large values of N, inequality (26) is reversed. Now, for the relevant time-scales, the function $P_1(t)$ has not approached it saturation value. In fact, in this case we can simplify the exponent in Eq. (17) by replacing the function $P_1(t)$ with its short-time approximation, see Refs. 30 and 38. We write

$$P_1(t) \approx P_1(0) + t\frac{dP_1(0)}{dt} = t\xi_1(0).$$

The value $\xi_1(0)$, the probability to transfer to state E from state 1 during the time-interval $(0, \Delta t)$ is known, see Eq. (19), $\xi_1(0) = \beta$. Using Eq. (17), we obtain

$$P_2(t) = 1 - \exp\left(-\frac{Nuu_1rt^2}{2}\right). \tag{33}$$

As expected, this is not a solution of system (12–14).

3. A SPATIAL MODEL

The models described above assume perfect mixing in the population of cells. There is no information about spatial locations, and no spatial dynamics. This may not be a shortcoming if we talk about liquid tumors (like leukemia). However in a discussion of solid tumors spatial considerations must play a role. Many spatial mechanistic models of cancer spread have been proposed (e.g., see the reviews 1–3, 7, 8). These are examples of a large body of literature on PDE-based spatial deterministic models. Such models typically do not take account of the evolutionary nature of cancer growth. The stochastic evolutionary nature of biological systems is now becoming of interest for the applied mathematics community, see e.g. Ref. 4. Here we concentrate on the stochastic aspect of evolutionary cellular dynamics of cancerous mutations.

As an attempt to include spatial considerations in the stochastic evolutionary dynamics of malignancy, we have designed a one-dimensional spatial generalization of the mass-action Moran birth-death process.[17] The cells are aligned along a regular grid, at locations $1, 2, \ldots, N$, see Fig. 2. As before, we assume that the total number of cells does not change. Cells are randomly chosen for death. Each cell death is followed by a cell division of one of its two neighboring cells, which places its daughter cell at the empty slot. Cell death occurs randomly and division is proportional to the relative fitness of the cells.

3.1. Two-Species Dynamics

As in Sec. 2.2, we first study diagram (2) with $u = 0$. Let us assume that there is a mutant cell with the relative fitness r at position j. The mutant cell produces mutant cells upon reproduction. Wild-type cells produce other wild type cells (the mutation rate is set to zero). If any cell at position $1, \ldots, j-2$ or $j+2, \ldots, N$ dies, then there can be no change in configuration. A change can occur only in two cases:

- Death occurs at position j, in which case the mutant disappears.
- Death occurs at position $j+1$ or $j-1$. Then the number of mutants can increase by one if the mutant cell is chosen for division.

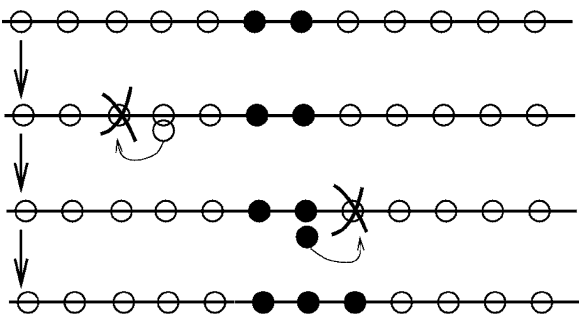

Fig. 2. The Moran process generalized to the one-dimensional space: a cell is chosen for death at random, and is immediately replaced by a division of one of the two neighboring cells (chosen proportional to their fitness).

Similarly, if we have several mutant cells at sequential positions from i through j, then a change of the number of mutants can only happen if death occurs at positions $i-1$, i, j or $j+1$(see Fig. 2). In this model, a mutant colony which originated as one cell can only occupy adjacent slots (a joint set). A change in the position of this set can only be caused by cell death at its boundary.

We can characterize the states of the system by positions of the leftmost and the rightmost mutants, i and j, such that

$$1 \leq i \leq j \leq N. \tag{34}$$

The transition matrix is given by the following. If the left boundary of the mutant domain is at 1 (or the right boundary is at N), then these boundaries cannot move anymore. Otherwise, if the number of mutants is larger than one, then the probabilities to expand the mutant domain to left and right are given by $P_{i,j\to i-1,j} = P_{i,j\to i,j+1} = \frac{1}{N}\frac{r}{1+r}$, and the probabilities to reduce the domain on left and right are given by $P_{i,j\to i+1,j} = P_{i,j\to i,j-1} = \frac{1}{N}\frac{1}{1+r}$. Finally, if there is only one mutant (that is, $i=j$), then we have $P_{i,i\to i-1,j} = P_{i,i\to i,i+1} = \frac{1}{N}\frac{1}{1+r}$, and the probability to lose the mutant is $\frac{1}{N}$. All the rest of the elements of the transition matrix are equal to zero.

We can envisage the dynamics as a 2-dimensional Markov random walk inside domain (34), with an additional absorbing state which can be reached from the diagonal $i=j$; this state corresponds to the extinction of the mutant and is denoted by $\tilde{E}$. The other absorbing state is the fixation of the mutant, $(0, N)$. The random walk is governed by the matrix above. We can set i to be the horizontal and j the vertical coordinate of the position of the walker, and then the above probabilities can be referred as $P_{ij}^{\rightarrow}$, $P_{ij}^{\leftarrow}$, $P_{ij}^{\uparrow}$ and $P_{ij}^{\downarrow}$.

3.2. Probability of Mutant Fixation

We can calculate the probability of absorption in $(0, N)$ starting from a state (i, j), which we call u_{ij}. We have the following system of equations,

$$
\begin{aligned}
u_{ij} &= u_{i-1,j}P^{\leftarrow} + u_{i+1,j}P^{\rightarrow} + u_{i,j-1}P^{\downarrow} + u_{i,j+1}P^{\uparrow} \\
&\quad + u_{ij}[1 - (P^{\leftarrow} + P^{\rightarrow} + P^{\downarrow} + P^{\uparrow})], \quad 1 < i < j < N, \\
u_{1j} &= u_{1,j+1}P^{\uparrow} + u_{1,j-1}P^{\downarrow} + u_{1j}[1 - (P^{\uparrow} + P^{\downarrow})], \quad 1 < j < N, \\
u_{1N} &= u_{i-1,N}P^{\leftarrow} + u_{i+1,N}P^{\rightarrow} + u_{iN}[1 - (P^{\leftarrow} + P^{\rightarrow})], \quad 1 < j < N, \\
u_{jj} &= u_{j-1,j}P^{\leftarrow} + u_{j,j+1}P^{\uparrow} + u_{jj}[1 - (P^{\leftarrow} + P^{\uparrow} + P^{\tilde{E}})], \quad 1 < j < N, \\
u_{11} &= u_{12}P^{\uparrow} + u_{11}[1 - (P^{\uparrow} + P^{\tilde{E}})], \qquad (35) \\
u_{NN} &= u_{N-1,N}P^{\leftarrow} + u_{NN}[1 - (P^{\leftarrow} + P^{\tilde{E}})], \qquad (36) \\
u_{1N} &= 1.
\end{aligned}
$$

The quantities u_{ii} are probabilities of fixation starting from one mutant at position i.

The results for this model must be compared with the probabilities of fixation in the mass-action model, Eqs. (6) and (7). Numerical solutions for the probabilities of absorption show that quantities u_{ii} are symmetric one-hump functions which are flat except for narrow boundary regions near $i = 1$ and $i = N$.[17] In order to find expressions for the "inner" values of fixation probabilities, we note the following. If point (i, j) is sufficiently far away from the boundary, then the boundary effects are not felt and u_{ij} only depends on $|j - i|$ rather than on the initial position of the mutant interval. In order to solve the problem away from the boundary, we can use the periodic boundary conditions, which is equivalent to replacing Eqs. (35) and (36) with the following:

$$u_{11} = u_{12}P^{\uparrow} + u_{11}[1 - (P^{\uparrow} + P^{\tilde{E}}/2)], \qquad (37)$$

$$u_{NN} = u_{N-1,N}P^{\leftarrow} + u_{NN}[1 - (P^{\leftarrow} + P^{\tilde{E}}/2)]. \qquad (38)$$

Now, quantities u_{ij} do not depend on the position of the mutant interval, but only on its length. Let us denote by π_j the probability that the mutant will reach fixation starting from a mutant interval of length $j + 1$. We have a self-consistent system of equations for the probabilities π_i,

$$\pi_1(P^{\uparrow} + P^{\downarrow}) = P^{\uparrow}\pi_{i+1} + P^{\downarrow}\pi_{i-1}, \quad 0 < i < N - 1, \qquad (39)$$

$$\pi_0(P^{\uparrow} + P^{\tilde{E}}/2) = P^{\uparrow}\pi_1, \qquad (40)$$

$$\pi_{N-1} = 1. \qquad (41)$$

This system can be solved by setting $\pi_i \propto \alpha^i$, and finding $\alpha = 1$ and $\alpha = P^{\downarrow}/P^{\uparrow} = 1/r$. Therefore, we have

$$\pi_i = A + B/r^i,$$

and the constants A and B are found from the boundary conditions,

$$A = \left(1 - \frac{r+1}{r^{N-1}(3r-1)}\right)^{-1}, \quad B = \frac{r^{N-1}(r+1)}{1+r+r^{N-1}-3r^N}.$$

The probability to reach fixation starting from only one mutant cell is given by $\rho_{\text{space}} \equiv \pi_0 = A + B$. We have,

$$\rho_{\text{space}} = \frac{2r^{N-1}(1-r)}{1+r+r^{N-1}-3r^N}.$$

We can compare this quantity with the fixation probability, ρ, in the mass-action model,

$$\rho_{\text{space}} = \rho \frac{2r(1-r^{N-1})}{1+r+r^{N-1}-3r^N}. \tag{42}$$

In particular, for neutral mutants such that $|r-1| \ll 1/N$, we have

$$\rho_{\text{space}} = \rho = 1/N.$$

For large values of N, we obtain, in the case of advantageous mutants ($r > 1, |r-1| \gg 1/N$),

$$\rho_{\text{space}} = \frac{2r}{3r-1}\rho < \rho, \tag{43}$$

and in the case of disadvantageous mutants ($r > 1, |1-r| \gg 1/N$) we have

$$\rho_{\text{space}} = \frac{2r}{1+r}\rho < \rho. \tag{44}$$

3.3. Three-Species Dynamics

Next, let us formulate the dynamics for a three-species model, diagram (1), in a one-dimensional space. Again, we will use a homogeneous state approximation, and describe the behavior of the system by means of Eqs. (12–14). The applicability conditions for this approximation are now somewhat more restrictive and they are derived in Sec. 3.4. The rate constants $R_{0\to 1}$ and $R_{1\to 2}$ can be calculated in the same way as for the non-spatial model. We have, instead of formula (15),

$$R_{0\to 1} = Nu\rho_{\text{space}} = Nu\frac{2r^N(1-r)}{1+r+r^N-3^{N+1}}, \tag{45}$$

where ρ_{space} is the probability of successful fixation of a mutant starting from one cell of type "B." Approximations for neutral and disadvantageous mutants are given by formulas (43) and (44). Similarly, we calculate the second rate in the two-step process, which is the same as in the mass-action model, Eq. (16),

$$R_{1\to 2} = Nu_1. \tag{46}$$

Finally, we need to find the tunneling rate, $R_{0\to 2}$.

3.4. The Tunneling Rate in the Spatial Model

In order to find the rate of tunneling, we again use the doubly-stochastic approximation, formula (17). Each (independent) lineage of type "B" spreads as a one-dimensional connected spot. The size of the spot is given by the random variable i. The state $i = 0$ is equivalent to the state $\tilde{E}$ of Sec. 3.1, i.e. the extinction of the mutant. The state $i = E$ corresponds to the creation of a mutant of type "C." The probability $P_1(t)$ in formula (17) is the probability to acquire a second mutation among the lineage of a single cell of type "B." Let us introduce a short-hand notation, $\tilde{r} = r/(r+1)$. Then for the dynamics within a lineage, the transition probabilities are given by: $P_{i\to i+1} = \tilde{r}(1-u_1)$ for $0 \le i \le N-1$, $P_{i\to i-1} = 1/(r+1)$ for $1 \le i \le N$, $P_{1\to 0} = 1/2$, $P_{N\to N} = N(1-u_1)$, $P_{i\to E} = 4\tilde{r}u_1 + (i-2)u_1$ for $3 \le i \le N$, $P_{2\to E} = 4\tilde{r}u_1$, and $P_{1\to E} = 2\tilde{r}u_1$, where time is measured in terms of generations. In what follows we will simplify the problem so that the transition probabilities are:

$$P_{i\to i+1} = \lambda, \quad P_{i\to i-1} = \mu, \quad P_{i\to E} = \beta i. \tag{47}$$

These are spatial analogues of formulas (18). Note that in formulas (18), the coefficients λ, μ and β were obtained by taking the lowest order term in the Taylor series in terms of the small i/N. In formula (47), the probabilities represent a "model" of the real situation rather than an approximation. Indeed, in Eqs. (47), with

$$\lambda = \tilde{r}(1-u_1), \quad \mu = 1/r(r+1), \quad \beta = 3\tilde{r}u_1,$$

we neglect several subtleties that we discovered for spatial propagation of mutants. For instance, we ignore the fact that $P_{1\to 0} \neq P_{i\to i-1}$ for $i > 1$. We also ignore the fact that the probability for exiting into state E from state i is not exactly proportional to i: for $i < 3$ it does not depend on i, and for larger i it has a constant (in i) term.

We will use the same method as we developed for the mass-action system. Let us denote by $\xi_i(t)\Delta t$ the probability to be absorbed in E during the interval $(t, t+\Delta t)$ starting from i at $t = 0$. We have the following equations for ξ_i:

$$\dot{\xi}_i = \lambda\xi_{i+1} + \mu\xi_{i-1} + \beta i\xi_E - (\lambda + \mu + \beta i), \quad 2 \le i,$$

with the boundary condition

$$\dot{\xi}_1 = \lambda\xi_2 + \mu\xi_0 + \beta\xi_E - (\lambda + \mu + \beta)\xi_1,$$

with $\xi_0 = \xi_E = 0$, and the initial condition

$$\xi_i(0) = i\beta.$$

The Laplace transform yields the system,

$$[\lambda f_{i+1} + \mu f_{i-1} - (\lambda + \mu + s) f_i] - f_i \beta i = -i\beta, \quad i > 1, \tag{48}$$

$$[\lambda f_2 - (\lambda + \mu + s) f_1] - f_1 \beta = -\beta. \tag{49}$$

This is similar to an inhomogeneous discrete Airy equation. Let us denote

$$h_i = f_i - 1,$$

and set $\mu = \lambda - \epsilon$. We have for the function h_i,

$$\lambda(h_{i+1} - 2h_i + h_{i-1}) + \epsilon(h_i - h_{i-1}) - s h_i = \beta i h_i, \tag{50}$$

$$\lambda(h_2 - h_1) - h_1(\lambda - \epsilon + \beta + s) = \lambda - \epsilon. \tag{51}$$

Using the continuous limit, we obtain the system

$$\lambda h'' + \epsilon h' - s h = \beta x h, \tag{52}$$

$$\lambda h'(0) - h(0)(\lambda - \epsilon + \beta + s) = \lambda - \epsilon; \tag{53}$$

for the second boundary condition we use the boundedness of the solution for large x. This system can be solved exactly in terms of the Airy function Ai and its derivative. Here we present the stationary solution corresponding to $s = 0$. We have

$$h(x) = \frac{2e^{-\epsilon x/(2\lambda)}(\epsilon - \lambda) Ai[K(x)]}{(2\beta - \epsilon + 2\lambda) Ai[K(0)] - 2\beta(\beta/\lambda)^{-2/3} Ai'[K(0)]},$$

$$K(x) = \frac{\epsilon^2 + 4\beta\lambda x}{4(\beta/\lambda)^{2/3}\lambda^2}.$$

Setting $x = 0$, we obtain

$$h(0) = \frac{2(\epsilon - \lambda)}{2\beta - \epsilon + 2\lambda - 2\beta(\beta/\lambda)^{-2/3} R\left(\left[\frac{\epsilon}{2\lambda(\beta/\lambda)^{1/3}}\right]^2\right)}, \quad R(z) = \frac{Ai'(z)}{Ai(z)}.$$

Depending on the fitness of type "B," this expression has a different limiting behavior. We consider these two cases:

- Type "B" is disadvantageous: $\epsilon < 0$ and $\epsilon \gg (\beta/\lambda)^{1/3}$. In this case, the argument of the function $R(z)$ tends to infinity and we can use the standard

asymptotic expansion of the Airy function and its derivative for a large argument. We obtain $h(0) = -1 + \frac{(\lambda-\mu)^2+\lambda^2}{(\lambda-\mu)^2\mu}\beta$, or $f(0) = 1 + h(0) =$

$$P_1^\infty = \frac{(\lambda-\mu)^2+\lambda^2}{(\lambda-\mu)^2\mu}\beta = 3ru_1\frac{(r-1)^2+r^2}{(r-1)^2}. \tag{54}$$

This rate has the same order of magnitude as the corresponding rate in the non-spatial calculation, Eq. (24).

- Type "B" is neutral, that is, $\epsilon \ll (\beta/\lambda)^{1/3}$. In this case, the argument of the function $R(z)$ tends to zero. We obtain

$$P_1^\infty = \left(\frac{3\beta}{\lambda}\right)^{1/3}\frac{\Gamma(2/3)}{\Gamma(1/3)} = (9u_1)^{1/3}\frac{\Gamma(2/3)}{\Gamma(1/3)}. \tag{55}$$

This rate is larger than the one found for the neutral mutant in the mass-action model, see expression (25).

Now we can calculate the tunneling rate. We will use the same method as in Sec. 2.4. Suppose t_c is the time where the function $P_1(t)$ comes close to its saturation value, P_1^∞ (the values for t_c are found in Ref. 17). Again, we will set the time-scale of the process such that the probability of acquiring a mutant of type "C" is of the order one. This is equivalent to the estimate $t \sim 1/(P_1^\infty uN)$, see Eq. (17). The condition $t \gg t_c$ will guarantee that the tunneling rate is simply uNP_1^∞. For the case of disadvantageous mutants, this condition is identical to

$$uN \ll \frac{r-1}{r+1}. \tag{56}$$

In the case of neutral mutants, we obtain

$$uN \ll \left(\frac{u_1}{3}\right)^{1/3}\left(\frac{\Gamma(1/3)}{\Gamma(2/3)}\right)^2\frac{r}{r+1}. \tag{57}$$

If these conditions are satisfied, then the tunneling rate, $R_{0\to 2} = NuP_1^\infty$ is given by

$$R_{0\to 2} = Nu\left[1 + \frac{2(\epsilon-\lambda)}{2\beta - \epsilon + 2\lambda - 2\beta(\beta/\lambda)^{-2/3}R\left(\left[\frac{\epsilon}{2\lambda(\beta/\lambda)^{1/3}}\right]^2\right)}\right],$$

$$R(z) = \frac{Ai'(z)}{Ai(z)}. \tag{58}$$

The limiting behavior is as follows:

- Type "B" is disadvantageous: $r < 1$ and $\frac{1-r}{1+r} \gg (3u_1)^{1/3}$. If condition (56) holds, then the tunneling rate is given by

$$R_{0\to 2} = 3rNuu_1 \frac{(r-1)^2 + r^2}{(r-1)^2}. \tag{59}$$

- Type "B" is neutral, that is, $\frac{1-r}{1+r} \ll (3u_1)^{1/3}$. If condition (57) holds, then the tunneling rate is given by

$$R_{0\to 2} = uN(9u_1)^{1/3} \frac{\Gamma(2/3)}{\Gamma(1/3)}. \tag{60}$$

Note that the rate of tunneling in the case of disadvantageous mutants, (59), is always larger than that for the mass-action model, Eq. (28). It has the same order of magnitude in terms of small u_1. Regarding the case of neutral mutants, it is interesting that the rate of tunneling in the spatial model, (60), has a *larger order of magnitude* than that in the mass-action model, Eq. (29). In both cases, tunneling happens faster in the spatial model compared to the mass-action model.

It is instructive to discuss the definition of neutrality in different models. It is the same for spatial and mass-action descriptions in the regime where a two-step process dominates (or if we have only two types, "A" and "B" in the system). In this case mutants with fitness satisfying $|1-r| \ll 1/N$ can be considered neutral. Indeed, in the expansion of the fixation probability of a mutant in terms of r around the value $r = 1$, the highest order term is given by $1/N$, and the next term is $(N-1)(r-1)/2N$ without spatial effects, and $(N-1)^2(r-1)/2N^2$ in the spatial model. The smallness of the second term compared to the first term is a criterion of neutrality.

The meaningful definition of neutrality changes in the regime where tunneling is important. There, it is not the time-scale of fixation, but rather the rate of tunneling which is the dominant factor. Now, the definition is different in the spatial model compared to that in the mass-action model. In the latter case, neutral mutants were defined by the condition

$$|1-r| \ll \sqrt{u_1}. \tag{61}$$

In the spatial case, we have

$$|1-r| \ll (3u_1)^{1/3}. \tag{62}$$

That is, a larger region of fitnesses around $r = 1$ qualifies as neutral.

The relative importance of tunneling can be obtained by comparing the rates $R_{0\to 1}$ and $R_{0\to 2}$. As in the mass-action model, condition (30) implies that typically, mutants of type "C" are generated before fixation of type "B" occurs.

For disadvantageous mutants of type "B," N_{tun} is given by

$$N_{\text{tun}} = \log\left[\frac{3}{2}\frac{u_1 r(r+1)[(r-1)^2+r^2]}{(r-1)^3}\right] \Big/ \log r. \tag{63}$$

In the case of neutral intermediate mutants, we have

$$N_{\text{tun}} = \frac{\Gamma(1/3)}{\Gamma(2/3)}\frac{1}{(9u_1)^{1/3}}, \tag{64}$$

to be compared with formula (32) for the mass-action model. We can see that N_{tun} is always smaller for the spatial model compared to that for the mass-action model.

Conditions (56) and (57) define whether the homogeneous state approximation holds. They are a stronger version of the conditions (9, 10) which were derived for the mass-action model. There, in order to be able to approximate the system by three long-lived states, it was enough to require that the first mutation rate is small compared to $1/N$. Now, an additional factor comes in. The conditions for applicability of system (12–14), inequalities (56) and (57), can be written as one condition,

$$N \ll N_{cg} = \frac{1}{u}\max\left\{\frac{1-r}{1+r}, (3u_1)^{1/3}\right\}. \tag{65}$$

3.5. Spatial Model: Beyond Tunneling

If condition (65) is violated, then the tunneling in this case happens according to a different scenario, and system (12–14) does not apply. In particular, for very large values of $N \gg N_{cg}$, the relevant time-scale is very small compared to the saturation time, t_c, and the function $P_1(t)$ can be approximated as a linear function of time, $P_1(t) \approx \xi_1(0)t$, in a way similar to Sec. 2.5. We have $\xi_1 = \beta$, and this gives us

$$P_2(t) = 1 - \exp\left(-\frac{3Nuu_1 r t^2}{2(r+1)}\right). \tag{66}$$

4. A HIERARCHICAL MODEL

Spatial locations are not the only factor determining the nature of cellular interactions and competition. Another important aspect is a hierarchical structure of cell populations.

This is indeed a common feature of many epithelial tissues. Some cells, called the progenitor, or stem, cells have a large proliferation capacity. Stem cells replenish the organ tissue by means of asymmetric divisions. Upon reproduction,

a stem cell gives rise to another stem cell, and a daughter cell with different properties. This asymmetric division pattern ensures that there is always a stem cell present which is kept as a "blueprint" throughout the life of the organism. Daughter cells (also called "partially differentiated cells," "transient cells," or "committed cells") divide symmetrically. Their division capacity is limited, that is, after a few divisions they become "fully differentiated," stop reproducing and eventually undergo apoptosis.

Here we will discuss a stochastic model of stem and daughter cell dynamics introduced by Ref. 20 and further developed by Ref. 18. Other models which distinguish between stem cells and differentiated daughter cells have also been analyzed.[5,28,32,39]

4.1. Model Description

Here we present a *finite branching process* model of epithelial cell turnover, which explicitly includes the processes of apoptosis, renewal, differentiation and mutation. In our model, we assume that cancerous mutations can be acquired in both stem and daughter cells, consistent with the thinking of Ref. 6.

Again we denote the total population size as N. For simplicity we will assume that there is only one stem cell; this assumption can be removed, see Ref. 18.

At each moment of time, there is exactly 1 stem cell and $N-1$ daughter cells, see Fig. 3. For each daughter cell, we keep track of how many divisions it has gone through. It is convenient to introduce the quantity l, the total number of division rounds before final differentiation. This number includes one asymmetric division of the stem cell and $l-1$ rounds of symmetric divisions of the daughter cells. After l divisions, a daughter cell is considered fully differentiated, and it is unable to divide further. For simplicity we assume that $N = 2^l$, that is, the number N is a power of 2. There is always one first generation daughter cell, two second generation daughter cells, $\ldots, 2^{l-1}$ daughter cells of generation l.

Let us set up the following process. At each (discrete) time-step, there are $N/2$ synchronized cell divisions; the dividing cells include the stem cells and all

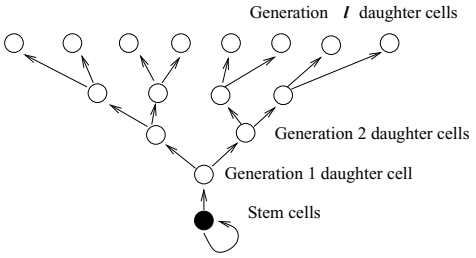

Fig. 3. A stem cell (black) gives rise to a branching tree of daughter cells.

the daughter cells except the fully-differentiated, generation l cells. The result of each stem cell division is a stem cell and a (first generation) daughter cell. The result of each daughter cell division is two daughter cells of the next generation. To keep the population size constant, the $N/2$ divisions are accompanied by $N/2$ deaths of the fully differentiated cells. Both stem and daughter cells can be of type "A," "B" and "C." At each cell division, there is a probability of mutation, according to diagram (1).

Note that in some sense this model is less general than the mass-action and spatial Moran processes described in the previous sections. Indeed, to preserve the hierarchical structure, we consider synchronized cell divisions, and restrict the value of the fitness of type "B" to $r = 1$. Positively and negatively selected intermediate mutants is a subject of future research.

4.2. Probability of Mutant Fixation in the Two-Species Model

The two-species model in this case can be defined, and the probability of mutant fixation can be obtained very simply. Indeed, if a daughter wild type cell undergoes a mutation, the mutants will be washed out after less than l cell divisions. However, if a mutation happens in the stem cell, then after l cell divisions, the entire population will be of type "B." Therefore, the probability of mutant fixation starting from one cell is equal to $1/N$. This result coincides with that for the mass-action and spatial models, in the case of neutral mutations ($r = 1$).

4.3. Three-Species Dynamics

Next, let us discuss the three-species model. As in the previous sections, we suppose x_0 is the probability that the whole population is wild type (type "A"). Similarly, x_1 is the probability to find the entire population consisting of single-mutants, type "B," and the probability to have at least one cell with a double mutation (type "C") is denoted by x_2. If the mutation rates are small compared to the inverse of the total population size, the inhomogeneity condition holds (see Ref. 19), and we have Eq. (11). This means that the system spends most of its time in the homogeneous states, and the transitions between them (when cells are of different types) are very fast.

Indeed, once the first hit has taken place in a stem cell, it takes only $\log_2 N$ cell divisions before the entire population becomes homogeneous with respect to the phenotype "B." This should be compared to the typical number of cell divisions before a mutation in a stem cell occurs, which is given by u^{-1}. Similarly, if the first hit occurs in one of the daughter cells, it takes less than $\log_2 N$ cell divisions before one of the two things happen: either the mutants are washed out, and the system returns to the wild-type state, or a second hit is acquired, which puts the system in the x_2 state. In fact, a stronger statement can be made: in the majority of

cases, a mutation in a daughter cell will happen only 1 or 2 steps away from either being shed off or converted to the "C" phenotype. Indeed, only $N/2^{k-1} - 1$ out of N cells are k steps or more away from being shed off. Therefore, the characteristic number of steps spent in a non-homogeneous state as a result of a first-hit mutation in a daughter cell is of the order one. This has to be compared with the typical waiting time until a mutation in one of the daughter cells is acquired, which is given by $[(N-1)u]^{-1}$. We can see that as long as

$$u \ll [N-1]^{-1}, \tag{67}$$

the transition $x_0 \to x_1$ is fast. In the same way we can reason that as long as

$$Nu_1 \ll 1, \tag{68}$$

the transition $x_1 \to x_2$ is fast. If these conditions hold, then the states x_0, x_1 and x_2 are long-lived, and the simplified, coarse-grained description, system (12–14), can be used.

Before we go on, we would like to give an intuitive interpretation of the dynamics of Eqs. (12–14) in the context of the hierarchical model. There are three ways in which mutations can be accumulated, see Fig. 4.

1. In the ss scenario (for "stem-stem," Fig. 4(a)), a mutation happens in the stem cell. Then, after a few divisions, the entire population will consist of mutated cells. At some point, a *second* mutation occurs in the stem cell, shortly after which the entire population will consist of double mutants.
2. In the sd scenario (for "stem-daughter," Fig. 4(b)), again a mutation occurs in the stem cell which then spreads throughout the population. However, the first double-mutant emerges in the proliferating/migrating compartment. This mutant divides and its progeny spreads in the upward direction.
3. In the dd scenario (for "daughter-daughter," Fig. 4(c)), a mutation occurs in one of the migrating daughter cells. The cell divides, its progeny moves in the upward direction, but before it is washed out, one of these cells experiences a second hit, creating a double mutant.

Scenarios ss and sd above are similar in spirit to the two step process of the mass-action model, Fig. 1(a), and scenario dd is equivalent to tunneling, Fig. 1(b).

Now, let us calculate the transition rates of system (12–14). We have,

$$R_{0\to 1} = u \tag{69}$$

is the rate of transition between states x_1 and x_2 and

$$R_{1\to 2} = Nu_1 \tag{70}$$

is the rate of transition between states x_1 and x_2. These rates describe cellular processes (1) and (2) above, which we call scenarios ss and sd. The third scenario, dd, happens at the rate $R_{0\to 2}$; this scenario takes place when both hits occur in

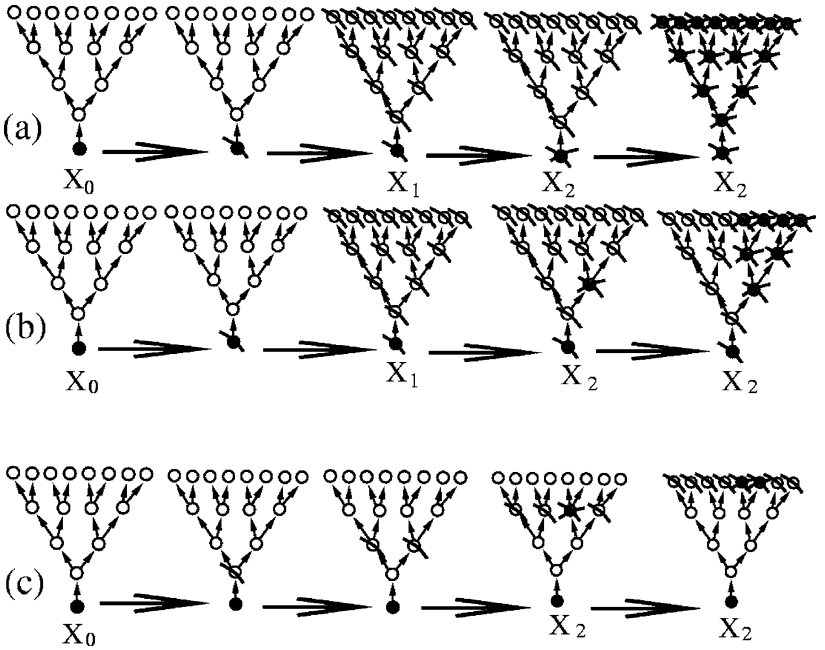

Fig. 4. The three scenarios of generating a double mutant. In these diagrams, the stem cells are marked as black circles. Cells containing a single mutation are denoted by circles crossed once. Double mutants are criss-crossed gray circles. (a) The *ss* scenario: both mutations occur in the stem cell. (b) The *sd* scenario: the first mutation happens in the stem cell and the second hit is acquired by one of the daughter cells. (c) The *dd* scenario: the first mutation hits one of the daughter cells, and before its progeny is shed away, the second mutation is acquired. For each scenario, the important states (x_0, x_1 and x_2) are marked.

a daughter cell, so a fixation in the x_1 state does not happen. Let us calculate the rate $R_{0\to 2}$.

4.4. The Tunneling Rate in the Hierarchical Model

To calculate the rate $R_{0\to 2}$, let us write down the probability to have at least one mutant such that both mutations happen in a daughter cell (given that no stem cell mutations have happened). We assume that the mutation rate, u, is sufficiently small such that the mutant clones can be treated independently (the condition is $uN \ll 1$), and consider a doubly stochastic process. Let us write down the total rate of primary mutations, $\sum_{i=1}^{l} u2^{i-1} = uN$. Then the contribution corresponding to the first mutation happening in a daughter cell of generation i is given by $r_i = u2^{i-1}$. Let us denote by $\mathcal{P}_i$ the probability to get a second hit in a "secondary" stochastic process which happens in the clone after the first mutation.

Inside such a clone, we have $2^{l-i+1}-2$ cell divisions, so that the total probability to get a second hit is

$$\mathcal{P}_i = 1-(1-u_1)^{2^{l-i+1}-2} \approx 1-e^{-u_1(2^{l-i+1}-2)}.$$

We obtain

$$R_{0\to 2} = \sum_{i=1}^{l} r_i \mathcal{P}_i,$$

which gives

$$R_{0\to 2} = u\sum_{i=1}^{l} 2^{i-1}(1-\exp[-u_1(2^{l-i+1}-2)]), \quad l=\log_2 N. \tag{71}$$

The expression for the tunneling rate, $R_{0\to 2}$, can be simplified. For instance, if we assume that $u_1 N \ll 1$, we can expand the expression under the summation sign in terms of this small parameter to obtain

$$R_{0\to 2} \approx uu_1[(\log_2 N-2)N+2].$$

This approximation works very well for small values of N, for all realistic values of u_1. However, if the quantity N is large, then this approximation breaks down for high values of the mutation rate, u_1. In this case it is convenient to replace the summation in Eq. (71) with an integral. Indeed, we can define $x=2^{i-1}/N$, and set formally $2^{i-1}\Delta i = \frac{N}{\log 2}\Delta x$. In the limit of very large N, this can be approximated by a differential, so that we have

$$R_{0\to 2} \approx \frac{uN}{\log 2}\left(\frac{1}{2}-\frac{1}{N}-e^{2u_1}\int_{\frac{1}{N}}^{\frac{1}{2}} e^{-u_1/x}dx\right). \tag{72}$$

The integral can be evaluated in terms of the incomplete Gamma function, $\Gamma(\alpha,z)=\int_z^\infty t^{\alpha-1}e^{-t}dt$:

$$R_{0\to 2} = \frac{ue^{2u}}{\log 2}[-e^{-2u_1}+e^{-Nu_1}+Nu_1(\Gamma(0,2u_1)-\Gamma(0,Nu_1))].$$

In the limit $Nu_1 \gg 1$ we have further simplifications:

$$R_{0\to 2} = \frac{Nuu_1}{\log 2}(|\log(2u_1)|-\gamma).$$

The relative contribution of the two-step and tunneling processes can be determined. Tunneling is the dominant process if $R_{0\to 1} \ll R_{0\to 2}$, which is equivalent to the condition $N \gg N_{\text{tun}}$, where $N=N_{\text{tun}}$ is the solution of equation $R_{0\to 2}=u$.

Note that under the condition $Nu_1 \gg 1$, this equation can be solved to yield

$$N_{\text{tun}} = \frac{\log 2}{u_1(|\log(2u_1)| - \gamma)}. \tag{73}$$

We can see that if condition (68) breaks down, then Eq. (73) holds, and moreover we have $N \gg N_{\text{tun}}$. This means that in this case, the main process is $x_0 \to x_2$, fixation in state x_1 never occurs, and condition (68) is in fact irrelevant. Therefore, we conclude that condition (67) is sufficient for validity of system (12–14):

$$N_{cg} = 1/u. \tag{74}$$

5. SUMMARY

In this paper we discussed stochastic cellular dynamics in populations with a constant number of cells, relevant to cancer initiation and progression. We concentrated on two important patterns. One is loss-of-function mutations characteristic of tumor suppressor gene inactivation, see diagram (1). The other is gain-of-function mutations, such as oncogene activation, see diagram (2).

We studied three models of cellular birth and death dynamics. In the mass-action model, initially all cells are identical (type "A"), and their properties do not depend on their spatial locations. A cell death is immediately followed by a cell division of a cell chosen at random, proportional to its fitness. The corresponding constant-population birth-death process is called the Moran process. In the spatial model, we keep track of spatial locations of cells on a one-dimensional regular grid. A dead cell in this model can only be replaced by the offspring of one of its neighbors. Finally, a hierarchical model includes a stem cell and daughter cells. The stem cell divides indefinitely and cannot die. For each daughter cell we keep track of the number of divisions it has gone through. After a fixed number of divisions, the daughter cell is destined to die.

5.1. Gain-of-Function Mutations

For gain-of-function mutations, we considered the dynamics of fixation of type "B," diagram (2). For all the models, the probability that the offspring of one cell of type "B" will reach fixation is given by $1/N$, as long as the fitness of type "B" is equal to that of type "A." If the fitness of type "B" is smaller or larger than that of type "A," then the probability of fixation is always bigger in the mass-action model compared to the spatial model, see Fig. 5.

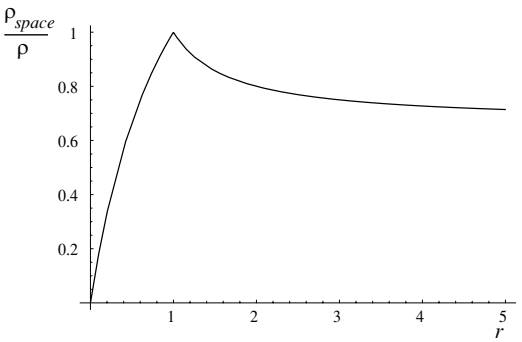

Fig. 5. The quantity ρ_{space}/ρ, formula (42), as a function of r for $N = 1000$. This quantity tells us how much less likely a mutant fixation is in the spatial model compared to the mass-action model.

5.2. Loss-of-Function Mutations

For loss-of-function mutations, we studied the dynamics of the acquisition of a second hit, diagram (1). Under certain conditions, the dynamics can be described by a coarse-grained system, (12–14), which represents Markovian hops between only three states. The first state is *all* "A," the second one is *all* "B" and the third one, *at least one cell of "C."* This simple description holds as long as N is not too large, $N \ll N_{cg}$, where the formulas for N_{cg} are given by Eqs. (10), (65) and (74) for the three models, respectively.

Within the region of applicability of system (12–14), we have two different regimes. If $N \ll N_{\text{tun}}$, then the dynamics is a genuine two-step process. First, there is a fixation of the intermediate mutant, "B," and only after that a cell of type "C" appears. The probability to have at least one cell of type "C" is given by

$$P_2(t) = 1 - \frac{R_{0\to 1}e^{-R_{1\to 2}t} - R_{1\to 2}e^{-R_{0\to 1}t}}{R_{0\to 1} - R_{1\to 2}}.$$

The values of the coefficients are as follows:

$$R_{0\to 1} = Nu\rho,$$

where ρ is the probability for type "B" to reach fixation starting from one cell; one should use ρ_{space} for the spatial model and $1/N$ for the neutral hierarchical model. We have $R_{1\to 2} = Nu_1$ for all models.

The value N_{tun} is calculated in Eqs. (31) and (32) for the mass-action model, Eqs. (63) and (64) for the spatial model and for the hierarchical model it is given implicitly by equation $R_{0\to 2} = u$ with $R_{0\to 2}$ in Eq. (71).

The second regime is defined by the inequality $N_{\text{tun}} \ll N \ll N_{cg}$. There, we have the process of tunneling, where the *all* "B" state never reaches fixation before a mutant of type "C" appears. In this regime, the probability of creation of a type

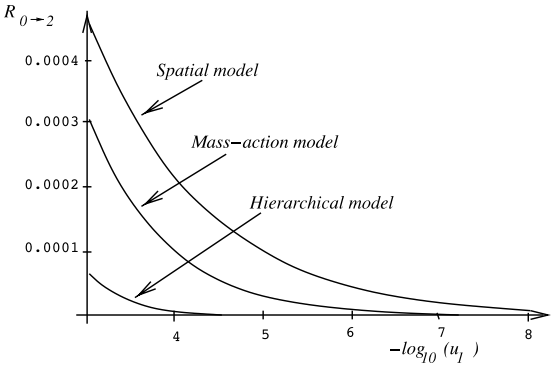

Fig. 6. The tunneling rate, $R_{0\to 2}$ as a function of u_1, for the three models. We assume that the intermediate mutants are neutral. The parameters are $N = 10^3$ and $u = 10^{-5}$.

"C" mutant is given by

$$P_2(t) = 1 - e^{-R_{0\to 2}t}.$$

The tunneling rate is given by Eq. (27) for the mass-action model; the simplified equations for the cases of neutral and disadvantageous mutants of type "B" are given by Eqs. (28) and (29). For the spatial model, $R_{0\to 2}$ is calculated in Eq. (58), and the limiting behavior is given by Eqs. (59) and (60). For the hierarchical model we have Eq. (71). All the rates (in the case of neutral mutants) are presented in Fig. 6. We can see that the rate of tunneling is the lowest in the hierarchical model, and the highest in the spatial model.

The different regions of behavior are shown in Fig. 7. Line 1 corresponds to N_{tun} for the spatial model, line 2 to N_{tun} for the mass-action model, line 3 to N_{cg} for the spatial model, line 4 - to N_{tun} for the hierarchical model, and line 5 to N_{cg} for the mass-action and the hierarchical models. For each of the models, we shaded the tunneling region, $N_{\text{tun}} < N < N_{cg}$. Below this region, we have a genuine two-step process, and above this region the coarse-grained description breaks down, resulting in behavior described by Eqs. (33) and (66) for the mass-action and spatial models.

5.3. Which Model Produces Mutants Faster?

The two-step process is characterized by two coefficients, $R_{0\to 1}$ and $R_{1\to 2}$. The value of $R_{1\to 2}$ is the same in all models. Let us compare the behavior of the mass-action and the spatial models. We have shown that the two-step rate, $R_{0\to 1}$, is larger the mass-action model (unless $r = 1$), and the tunneling rate $R_{0\to 2}$ is always larger in the spatial model. The question is, in which model does the first mutant of type "C" appear faster?

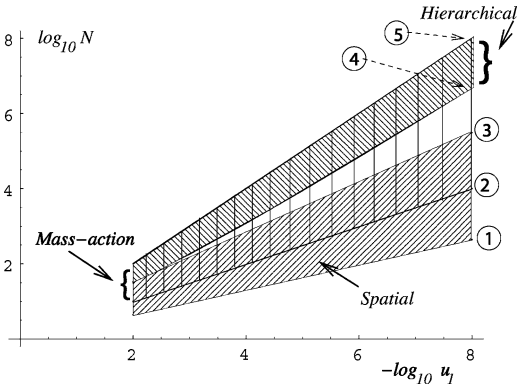

Fig. 7. Tunneling regions for the three models, under the assumptions $u = u_1$ and $r = 1$. The region with a right-slanted pattern corresponds to the spatial model, the region with a left-slanted pattern—to the hierarchical model, and the vertical stripes to the mass-action model. For each model, the values of N below the patterned region correspond to a genuine two-step process. For values of N above the patterned region coarse-grained description (12–14) breaks down, and we have Eqs. (33) and (66).

The following results are obtained readily from our theory. In the case of neutral intermediate mutants (Fig. 7), the system is in the tunneling regime between lines 2 and 3, for both mass-action and spatial models. In this regime, the spatial model produces mutants of type "C" faster. Below line 1, both models are in the two-step regime, and there the rates are the same, so there is not much difference between the two models. If the intermediate mutant is disadvantageous (not shown), then for low values of N (the two-step regime), the mass-action model will generate "C" mutants faster.

Next, let us compare the behavior of the hierarchical and mass-action models. The rate $R_{0\to 1}$ is the same, and the tunneling rate is larger in the mass-action model, Fig. 6. Below line 2 in Fig. 7, both models behave similarly, as tunneling does not make a significant contribution in that regime. Between lines 4 and 5, both models are in the tunneling regime, and the mass-action model will produce mutants faster. Between lines 2 and 4, the mass-action model functions in the tunneling regime, while the hierarchical model is still in the two-step mode. Therefore, the mass-action model will be characterized by a faster rate of producing "C."

Finally, we can compare the hierarchical and spatial models. Below line 1, both models are in the two-step regime, and both models act similar to one another. Between lines 1 and 3, the spatial model is in the tunneling regime, and it will produce mutants a lot faster. Note that line 3, the value N_{cg}, depends on u. If we assume that $u < u_1$, then line 3 will move up and the region where we can compare the two models will be larger. In any case, between lines 3 and 5, the spatial model produces double-mutants according to law (66), while the hierarchical model is either in a two-step, or in a tunneling regime with a comparatively low rate of

tunneling. We conclude that in the region, the spatial model generates mutants faster.

6. DISCUSSION

We have shown that stochastic cellular dynamics of mutation-selection diagrams (1) and (2) strongly depend on the details of modeling. For advantageous or disadvantageous gain-of-function mutations, the probability of fixation is lower in the spatial model. It is the same in all three models for neutral mutations.

For loss-of-function mutations with neutral intermediate mutants, there is not much difference among the models as long as the population size is smaller than N_{tun} in the spatial model, see formula (64) or line 1 in Fig. 7. However, for larger population sizes, the spatial model is characterized by the fastest production of double mutants, followed by the mass-action model. For disadvantageous intermediate mutants, the spatial model is the slowest for low values of N (lower than N_{tun} given by (63)); it is again the fastest for larger values of N.

The difference in the predictions of the three models can be quite substantial. For instance, if we take $u = u_1 = 10^{-5}$ and $N = 10^4$, after 100 generations the probability to have started a colony of type "C" is given by $p_h = 2 \times 10^{-3}$ in the hierarchical model, $p_{m-a} = 3 \times 10^{-2}$ in the mass-action model and $p_{sp} = 2 \times 10^{-1}$ in the spatial model. For parameter values $u = u_1 = 10^{-6}$, and the same colony size, we have after 1000 generations: $p_h = 10^{-3}$, $p_{m-a} = 10^{-2}$ and $p_{sp} = 10^{-1}$. We can see that the three models result in an order-of-magnitude difference in their predictions. One could envisage the following experiment where these calculations can be verified. Suppose we have a cell culture where space is a limiting factor such that the cells are in competition with each other. Various degrees of cellular mixing can be attained by putting cells in different environments. Suppose all cells are of type "A" at the beginning, and type "C" cells are marked for an easy detection (e.g. with GFP, the green fluorescent protein). After a fixed number of generations, we can determine the number of cultures which developed clones of type "C" cells. This should be compared with the quantities p_{m-a}, p_{sp} and p_h to see which model gives a better fit.

A lesson that we learn from the three models analyzed in this paper is that both space and cellular hierarchy are important. Therefore, one must be cautious and instead of using the simplest, mass-action model, examine carefully if the spatial or hierarchical considerations should be included. For instance, when modeling the initiation of cancers of the blood, spatial considerations do not enter in the same way as in solid tissues, while cellular hierarchy is definitely present; therefore, the hierarchical model must be implemented. In solid tumors during latent periods before a clonal expansion, cellular hierarchy may be unimportant but spatial consideration must be taken into account, thus making the spatial model the tool of choice.

An important area of applications of multistage models of the kind presented here, is the comparison with epidemiological data. Starting with early studies of Knudson[16] until recent works of Moolgavkar and his group,[10,11,26,27] two-hit and multi-hit models have been compared with age-incidence data on various cancers. Usually, the goal of such research is to derive unknown system parameters from fitting the model results with the age-incidence curves. There, the difference between the three models can become very important.

Apart from this, our results also allow us to speculate about various types of tissue architecture and its protective role against cancer. There are different ways of keeping a cell population constant (homeostatic control). We have discussed three ways of maintaining a constant cell number while allowing a cellular turnover.

In particular, we have shown that a hierarchical structure of tissue where a small number of stem cells divide indefinitely and daughter cells only undergo a limited number of divisions, minimizes the risk of generation of double mutants, compared to homogeneous cellular populations. This is consistent with hierarchical tissue architecture of epithelial tissues such as colon, breast, and skin, and other tissues such as blood. One of the reasons of such hierarchical tissue organization may be that it lowers the risk of cancerous transformations.

Another interesting result concerns the spatial model. We have shown that for cellular populations more than roughly 10^2, a spatial organization of cells increases the rate of double mutant generation. We would like to discuss the mathematical reasons for this result and also its possible implications. The reason for this accelerated rate of double-mutant production compared to the mass-action model is the very slow dynamics of single mutant cells. Let us look at the rate at which the number of mutants of type "B" can decrease/increase in the two models, see Eqs. (18) and (47). We notice that for the mass-action model, these rates are larger as long as the number of mutants is greater than one. Indeed, in the spatial model, cells of type "B," once produced, form mutant "islands," i.e. joint sets of points of type "B." The number of mutants can only change if a death occurs at one of the two boundaries of such islands. In the mass-action model, a change in the mutant number can occur upon death of any cell, followed by a reproduction of any cell of the other type. Therefore, in the spatial model, once an island of type "B" mutants is created, it tends to linger for a long time, serving as a platform for creating a double mutant.

We can see that the feature of the spatial model that a cell can only be replaced by an offspring of its immediate neighbor, creates the problem of long-lived mutant islands, which leads to very high tunneling rates of creating double mutants. The same conclusions will hold for two-dimensional and three-dimensional generalizations of the model. Therefore, this particular way of homeostatic control seems suboptimal. Instead, one can relax the assumption that the cells cannot move and can only reproduce if there is a dead cell right next to them. We could generalize this model such that upon a cell death, there is a nonzero probability of

reproduction not only for its two neighbors, but also for cells k slots away from it. This model will have properties intermediate between the mass-action model and the spatial model discussed here, and it will be characterized by lower tunneling rates compared to the first spatial model. Biologically this means that increased cellular motility and nonlocal cellular interactions can play a protective role against cancer.

Finally, we would like to describe an experimental setup which can be used to check the predictions of the models and to extend and improve the spatial model. It has been shown analytically that one of important components of the dynamics of tumor-suppressor gene inactivation is stochastic tunneling. In order to measure the intensity of tunneling, one could experimentally determine the frequency, size and average life-span of type-"B" mutant "islands" that appear in a constant-population culture. Such measurements can be related to the mathematical predictions for the tunneling rate, and, even more importantly, this information can be used to formulate two- and three-dimensional spatial stochastic models of cellular dynamics.

REFERENCES

1. R. Araujo and D. McElwain, A history of the study of solid tumor growth: The contribution of mathematical modeling. *Bull. Math Biol.* **66**(5):1039–1091 (2004).
2. N. Bellomo, A. Bellouquid and M. Delitala, Mathematical topics in the modeling complex multicellular systems and tumor immune cells competition. *Math. Mod. Meth. Appl. Sci.* **14**:1683–1733 (2004).
3. N. Bellomo and L. Preziosi, Modeling and mathematical problems related to tumor evolution and its interation with the immune system. *Math. Comp. Modeling* **22**(3–4):413–452 (2000).
4. A. Bellouquid and B. Delitala, Mathematical methods and tools of kinetic theory towards modelling complex biological systems. *Math. Mod. Meth. Appl. Sci.* **15**:1639–1666 (2005).
5. M. Bjerknes, Expansion of mutant stem cell populations in the human colon. *J. Theor. Biol.* **178**(4):381–385 (1996).
6. J. Cairns, Mutation selection and the natural history of cancer. *Nature* **255**(5505):197–200 (1975).
7. M. Chaplain, Avascular growth, angiogenesis and vascular growth in solid tumors. *Math. Comp. Modeling* **23**(6):47–87 (1996).
8. M. Chaplain and G. Lolas, Spatio-temporal heterogeneity arising in a mathematical model of cancer invasion of tissue. *Math. Mod. Meth. Appl. Sci.* **15**:1685–1734 (2005).
9. A. Dewanji, S. H. Moolgavkar and E. G. Luebeck, Two-mutation model for carcinogenesis: joint analysis of premalignant and malignant lesions. *Math. Biosci.* **104**(1):97–109 (1991).
10. W. D. Hazelton, M, S. Clements and S. H. Moolgavkar, Multistage carcinogenesis and lung cancer mortality in three cohorts. *Cancer Epidemiol. Biomarkers Prev.* **14**(5):1171–1181 (2005).
11. W. F. Heidenreich, E. G. Luebeck, W. D. Hazelton, H. G. Paretzke and S. H. Moolgavkar, Multistage models and the incidence of cancer in the cohort of atomic bomb survivors. *Radiat. Res.* **158**(5):607–614 (2002).
12. W. F. Heidenreich, E. G. Luebeck and S. H. Moolgavkar, Some properties of the hazard function of the two-mutation clonal expansion model. *Risk Anal.* **17**(3):391–399 (1997).
13. N. Heisterkamp, K. Stam, J. Groffen, A. de Klein and G. Grosveld, Structural organization of the bcr gene and its role in the Ph' translocation. *Nature* **315**(6022):758–761 (1985).

14. Y. Iwasa, F. Michor and M. A. Nowak, Stochastic tunnels in evolutionary dynamics. *Genetics* **166**(3):1571–1579 (2004).
15. S. Karlin and H. Taylor, *A First Course in Stochastic Processes, Second Edition* (Academic Press, New York, 1975).
16. A. G. J. Knudson, Mutation and cancer: statistical study of retinoblastoma. *Proc. Natl. Acad. Sci. USA* **68**(4):820–823 (1971).
17. N. Komarova, Spatial stochastic models for cancer initiation and progression. *Bull. Math. Biol.*, DOI: 10.1007/s11538-005-9046-8:1–27 (2006).
18. N. Komarova and P. Cheng, Epithelial tissue architecture protects against cancer. *Math. Biosci.* **200**(1):90–117 (2006).
19. N. L. Komarova, A. Sengupta and M. A. Nowak, Mutation-selection networks of cancer initiation: tumor suppressor genes and chromosomal instability. *J. Theor. Biol.* **223**(4):433–450 (2003).
20. N. L. Komarova and L. Wang, Initiation of colorectal cancer: Where do the two hits hit? *Cell Cycle* **3**(12):1558–1565 (2004).
21. N. L. Komarova and D. Wodarz, The optimal rate of chromosome loss for the inactivation of tumor suppressor genes in cancer. *Proc. Natl. Acad. Sci. USA* **101**(18):7017–7021 (2004).
22. C. Lengauer, K. W. Kinzler and B. Vogelstein, Genetic instabilities in human cancers. *Nature* **396**(6712):643–649 (1998).
23. M. P. Little and E. G. Wright, A stochastic carcinogenesis model incorporating genomic instability fitted to colon cancer data. *Math. Biosci.* **183**(2):111–134 (2003).
24. L. A. Loeb, Mutator phenotype may be required for multistage carcinogenesis. *Cancer Res.* **51**(12):3075–3079 (1991).
25. L. A. Loeb, A mutator phenotype in cancer. *Cancer Res.* **61**(8):3230–3239 (2001).
26. E. G. Luebeck, W. F. Heidenreich, W. D. Hazelton, H. G. Paretzke and S. H. Moolgavkar. Biologically based analysis of the data for the Colorado uranium miners cohort: age, dose and dose-rate effects. *Radiat. Res.* **152**(4):339–351 (1999).
27. E. G. Luebeck and S. H. Moolgavkar, Multistage carcinogenesis and the incidence of colorectal cancer. *Proc. Natl. Acad. Sci. USA* **99**(23):15095–15100 (2002).
28. F. Michor, Y. Iwasa, H. Rajagopalan, C. Lengauer and M. A. Nowak, Linear model of colon cancer initiation. *Cell Cycle* **3**(3):358–362 (2004).
29. S. H. Moolgavkar, The multistage theory of carcinogenesis and the age distribution of cancer in man. *J. Natl. Cancer Inst.* **61**(1):49–52 (1978).
30. M. A. Nowak, F. Michor, N. L. Komarova and Y. Iwasa, Evolutionary dynamics of tumor suppressor gene inactivation. *Proc. Natl. Acad. Sci. USA* **101**(29):10635–10638 (2004).
31. E. Parzen, *Stochastic Processes*, vol. 24 of *Classics in Applied Mathematics* (SIAM, 1999).
32. S. Ro and B. Rannala, Methylation patterns and mathematical models reveal dynamics of stem cell turnover in the human colon. *Proc. Natl. Acad. Sci. USA* **98**(19):10519–10521 (2001). Comment.
33. T. Strachan and A. P. Read, *Human Molecular Genetics 2* (John Wiley & Sons, Inc., 1999).
34. W. Y. Tan, *Stochastic Models of Carcinogenesis* (Marcel Drekker, New York, 1991).
35. W. Y. Tan and C. W. Chen, Stochastic models of carcinogenesis, some new insight. *Math. Comput. Modeling* **28**:49–71 (1998).
36. B. Vogelstein and K. W. Kinzler, *The Genetic Basis of Human Cancer* (McGraw-Hill, 1997).
37. B. Vogelstein and K. W. Kinzler, Cancer genes and the pathways they control. *Nat. Med.* **10**(8):789–799 (2004).
38. D. Wodarz and N. Kornarova, *Computational Biology of Cancer: Lecture Notes and Mathematical Modeling* (World Scientific, 2005).
39. Y. Yatabe, S. Tavare and D. Shibata, Investigating stem cells in human colon by using methylation patterns. *Proc. Natl. Acad. Sci. USA* **98**(19):10839–10844 (2001).